Ornstein-Zernike equation and Percus-Yevick theory for molecular crystals

Michael Ricker* and Rolf Schilling†
Institut für Physik, Johannes Gutenberg-Universität Mainz, Staudinger Weg 7, D-55099 Mainz, Germany
(Received 4 November 2003; revised manuscript received 23 January 2004; published 16 June 2004)

We derive the Ornstein-Zernike equation for molecular crystals of axially symmetric particles and apply the Percus-Yevick approximation. The one-particle orientational distribution function $\rho^{(1)}(\Omega)$ has a nontrivial dependence on the orientation Ω, in contrast to a liquid, and is needed as an input. Despite some differences, the Ornstein-Zernike equation for molecular crystals has a similar structure as for liquids. We solve both equations numerically for hard ellipsoids of revolution on a simple cubic lattice. Compared to molecular liquids, the orientational correlators in direct and reciprocal space exhibit less structure. However, depending on the lengths a and b of the rotation axis and the perpendicular axes of the ellipsoids, respectively, different behavior is found. For oblate and prolate ellipsoids with $b \gtrsim 0.35$ (in units of the lattice constant), damped oscillations in distinct directions of direct space occur for some of the orientational correlators. They manifest themselves in some of the correlators in reciprocal space as a maximum at the Brillouin zone edge, accompanied by a maximum at the zone center for other correlators. The oscillations indicate alternating orientational fluctuations, while the maxima at the zone center originate from ferrorotational fluctuations. For $a \lesssim 2.5$ and $b \lesssim 0.35$, the oscillations are weaker, leading to no marked maxima at the Brillouin zone edge. For $a \gtrsim 3.0$ and $b \lesssim 0.35$, no oscillations occur any longer. For many of the orientational correlators in reciprocal space, an increase of a at fixed b or vice versa leads to a divergence at the zone center $\mathbf{q}=\mathbf{0}$, consistent with the formation of ferrorotational long-range fluctuations, and for some oblate and prolate systems with $b \lesssim 1.0$ a simultaneous tendency to divergence of few other correlators at the zone edge is observed. Comparison of the orientational correlators with those from Monte Carlo simulations shows satisfactory agreement. From these simulations we also obtain a phase boundary in the a-b plane for order-disorder transitions.

DOI: 10.1103/PhysRevE.69.061105 PACS number(s): 64.10.+h, 61.43.−j, 64.70.Kb

I. INTRODUCTION

The experimental, numerical, and analytical study of structural properties of simple liquids is a well established discipline of condensed matter physics. In the center of such investigations is the static structure factor $S(q)$. There are powerful integral equations allowing an approximate calculation of $S(q)$ [1]. The starting point is the Ornstein-Zernike (OZ) equation, relating the total correlation function $h(q)$ and the direct correlation function $c(q)$. An additional closure relation, such as the Percus-Yevick (PY) approximation, then allows to determine $h(q)$, from which $S(q)$ follows from

$$S(q) = 1 + \rho h(q), \tag{1}$$

where ρ is the number density of the liquid. Application of the PY approximation to a liquid of hard spheres yields good agreement with the exact result for intermediate values of ρ [1]. However, the crystallization of hard spheres cannot be described by PY theory.

The extension of the OZ equation and the PY approximation (or other closure relations) to molecular liquids is straightforward [1,2] and has been applied extensively (see, e.g., Refs. [3,4]). As for simple liquids, PY theory usually does not yield an order-disorder phase transition. Therefore, it was quite surprizing that a recent application of the molecular version of that theory to a liquid of hard ellipsoids of revolution with aspect ratio X_0 has allowed the location of a phase boundary in the ρ -X_0 plane, at which a transition to a nematic phase takes place [4].

Much less analytical work exists for molecular crystals [5,6]. These are crystalline materials with, e.g., a molecule at each lattice site. One of the main interest concerns phase transitions of the translational and rotational degrees of freedom (see, e.g., the review Ref. [7]). These transitions are influenced by the translation-rotation coupling [8]. But phase transitions also exist if the crystal is assumed to be rigid. This has been shown a long time ago by use of the mean-field approximation (see, e.g., Refs. [9–11]). Most of this work is devoted to real molecules like CH_4, CD_4, etc. If the size of the molecules is much larger than the lattice constant, there will be strong steric hindrance. In an idealized way, one may replace the soft pair potentials by hard body interactions. This will be done in the present paper. We will consider hard ellipsoids of revolution with their centers at the lattice sites of a simple cubic lattice with lattice constant equal to one. The lengths of the rotation axis and the perpendicular axes of the ellipsoids are a and b, respectively. This is an athermal system for which the free energy is given by $F=-TS$, i.e., a phase transition can only be induced by the entropy S. Similar to hard spheres (see, e.g., Ref. [12]) we expect a phase transition to an orientationally ordered phase due to entropic effects. That such an ordered phase may occur can be intuitively understood as follows. If for given b the length a is large enough, i.e., the volume fraction is large enough, an orientationally *disordered* phase is characterized by many ellipsoids in contact with each other. Accordingly,

*Electronic address: mricker@uni-mainz.de
†Electronic address: rschill@uni-mainz.de

the free volume of the ellipsoids, i.e., the average solid angle an ellipsoid can rotate freely, is small. However, if the ellipsoids are *ordered* they may be less blocked in certain orientational directions, thereby gaining free volume. Since the entropy is proportional to the logarithm of the free volume, it will be larger for the ordered phase, leading to a lower free energy F. From this argument we expect a phase transition to an orientationally ordered phase at a critical length $a_c(b)$.

Besides phase transitions, the study of the orientational structure of molecules on a rigid lattice is of interest, too. Changing temperature will influence the steric hindrance between the molecules. The same happens for hard ellipsoids when changing a and b. Analogous to simple and molecular liquids, one can quantify such static orientational properties by the one-particle orientational distribution function $\rho^{(1)}(\Omega)$ [6,8,13–15] and by the orientational correlation function $G_{nn'}(\Omega,\Omega')$ of molecules at sites n and n', where the orientation Ω can be characterized, e.g., by the Euler angles (ϕ,θ,χ) or, for axially symmetric particles, by (ϕ,θ). Then the following questions arise: How to compute $\rho^{(1)}(\Omega)$ and, above all, the correlation function $G_{nn'}(\Omega,\Omega')$ by an analytical method? Does the result for $G_{nn'}(\Omega,\Omega')$ allows to locate a phase boundary where a transition to an orientationally ordered phase occurs? To provide answers to these questions is the main motivation of our contribution

There already exist theoretical approaches to these questions. For example, discretizing the angular degrees of freedom, the orientational correlators and finally the neutron scattering cross section were calculated by use of a cluster expansion [16] and by a mean-field type of approximation [17]. The critical diffuse scattering was described by an OZ approximation (mean-field approximation) of the corresponding susceptibility [18,19]. In the present paper we will provide answers to the questions above by following quite a *different strategy*. We will extend the powerful methods for calculating the static correlation functions for simple and molecular liquids to molecular crystals. To be more specific, we will derive the OZ equation for molecular crystals and will use the PY approximation as a closure condition.

Our paper is organized as follows. In Sec. II we will introduce the model and the basic physical quantities such as the one-particle distribution function $\rho^{(1)}(\Omega)$ and the orientational correlation function $G_{nn'}(\Omega,\Omega')$. The analytical approach of calculating $G_{nn'}(\Omega,\Omega')$ or its transform $S_{\lambda\lambda'}(\mathbf{q})$ from the OZ equation in combination with the PY approximation is described in Sec. III. Results from PY theory for hard ellipsoids of revolution on a simple cubic lattice will be shown in Sec. IV and compared with those from Monte Carlo (MC) simulations. This section also presents a short discussion of the phase transition for the ellipsoids from an orientationally disordered to an ordered phase. The final Sec. V contains a discussion of the results and some conclusions. We add three appendixes, including extensive technical manipulations needed in Secs. III and IV.

II. DISTRIBUTION AND CORRELATION FUNCTIONS

We consider a three-dimensional periodic lattice with N lattice sites and periodic boundary conditions. If the nth lattice site has the position $\mathbf{x}_n$, the difference between two sites is the vector $\mathbf{x}_{nn'}=\mathbf{x}_{n'}-\mathbf{x}_n$. We assume the lattice to be rigid with lattice constant equal to one. At each lattice site we fix a rigid molecule, not necessarily with its center of mass. Restricting to linear molecules, the orientation of the molecule at site n is given by $\Omega_n=(\phi_n,\theta_n)$. The third Euler angle χ_n is irrelevant for our purposes. Extension of our theoretical approach below to arbitrary molecules is straightforward. The interaction energy $V(\{\Omega_n\})$ is assumed to be pairwise and the classical Hamiltonian is given by

$$H(\{\Omega_n\},\{\mathbf{l}_n\}) = \sum_{n=1}^{N} \frac{1}{2}\mathbf{l}_n^T\,\mathbf{I}^{-1}(\Omega_n)\mathbf{l}_n + V(\{\Omega_n\}), \tag{2}$$

where $\mathbf{l}_n$ and $\mathbf{I}(\Omega_n)$, respectively, are the angular momentum and the tensor of inertia of the molecule at site n in the space fixed frame. Since we will investigate static quantities only, the kinetic part of $H(\{\Omega_n\},\{\mathbf{l}_n\})$ does not matter.

In order to describe the orientational degrees of freedom, we introduce the microscopic one-particle density $\rho_n(\Omega)$ at lattice site n and its associated fluctuation $\delta\rho_n(\Omega)$ defined by

$$\rho_n(\Omega) = \delta(\Omega|\Omega_n), \tag{3a}$$

$$\delta\rho_n(\Omega) = \rho_n(\Omega) - \langle\rho_n(\Omega)\rangle, \tag{3b}$$

where $\delta(\Omega|\Omega')=(\sin\theta)^{-1}\,\delta(\theta-\theta')\delta(\phi-\phi')$. $\langle(\cdot)\rangle$ denotes canonical averaging with respect to $H(\{\Omega_n\},\{\mathbf{l}_n\})$. Note that the Ω_n dependence of ρ_n and $\delta\rho_n$ is suppressed. The one-particle orientational distribution function is given by

$$\rho^{(1)}(\Omega) = \langle\rho_n(\Omega)\rangle, \tag{4}$$

which is n independent due to the lattice translational invariance of $H(\{\Omega_n\},\{\mathbf{l}_n\})$, and the two-particle distribution is defined as

$$\rho^{(2)}_{nn'}(\Omega,\Omega') = \langle\rho_n(\Omega)\rho_{n'}(\Omega')\rangle \quad (n\neq n'). \tag{5}$$

Making use of Eqs. (3), it follows that

$$\int_{S^2} \rho^{(1)}(\Omega)d\Omega = 1, \tag{6}$$

$$\int_{S^2} \rho^{(2)}_{nn'}(\Omega,\Omega')d\Omega = \rho^{(1)}(\Omega') \quad (n\neq n'), \tag{7a}$$

$$\int_{S^2} \rho^{(2)}_{nn'}(\Omega,\Omega')d\Omega' = \rho^{(1)}(\Omega) \quad (n\neq n'). \tag{7b}$$

where the integrations are done over S^2, the surface of the unit sphere. $\rho^{(1)}(\Omega)$ is similarly obtained from $\rho^{(2)}_{nn'}(\Omega,\Omega')$ as the crystal field is deduced from the pair potential [9–11]. However, $\rho^{(1)}(\Omega)$ is not only determined from the crystal field but also from the (Ω,Ω')-dependent part of the potential.

It is important to realize that in contrast to isotropic molecular liquids the one-particle distribution function $\rho^{(1)}(\Omega)$ depends on Ω. Here a comment is in order. In case of *hard*

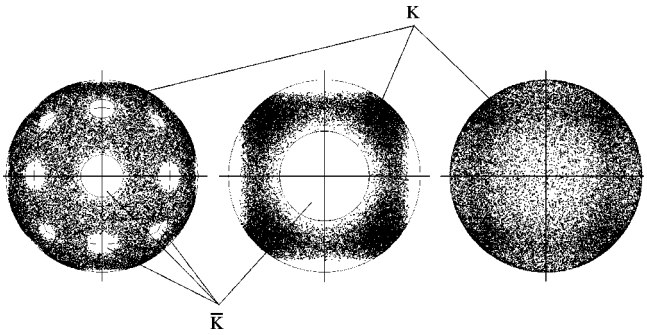

FIG. 1. MC results for $\rho^{(1)}(\Omega)$ for hard ellipsoids of revolution with $a=3.6$, $b=0.24$ (left), $a=1.2$, $b=0.88$ (middle), and $a=0.56$, $b=1.1$ (right) on a simple cubic lattice. Orientations on S^2 obtained from MC runs are projected along the fourfold lattice direction. Parts of $\overline{K}$ occur along the twofold, threefold and fourfold lattice directions, depending approximately on whether $(a+b)/2$ exceeds the site-site spacing along one of these directions. Some circles approximating the edges of the parts of $\overline{K}$ are shown as an aid for the eye.

body potentials there may exist regions (denoted by $\overline{K}$) on S^2 in which the hard particles overlap such that $\rho^{(1)}(\Omega)$ and $\rho^{(2)}_{nn'}(\Omega,\Omega')$ vanish. Accordingly, these distribution functions are nonzero on the complement K of $\overline{K}$, only. An illustration is given in Fig. 1. The restriction of Ω to allowed regions has led the authors of Refs. [16] and [17] even to approximate the components of K by a *finite* number of discrete orientations. The vanishing of $\rho^{(1)}(\Omega)$ and $\rho^{(2)}_{nn'}(\Omega,\Omega')$ on $\overline{K}$ introduces some technical problems (see below). But fortunately one can prove that the equations derived for *soft potentials* can be used to calculate the orientational correlators for hard body interactions [20], what will be done here. This is plausible, since approximating a hard potential by a sequence of soft potentials becoming harder and harder, one expects that the corresponding orientational correlators converge to those for the hard potential.

Next, we introduce the orientational density-density correlation function $G_{nn'}(\Omega,\Omega')$. It describes the correlation of the fluctuations of $\rho_n(\Omega)$ at lattice sites n and n',

$$G_{nn'}(\Omega,\Omega') = \langle \delta\rho_n(\Omega)\,\delta\rho_{n'}(\Omega')\rangle. \tag{8}$$

By use of Eqs. (3)–(5) we get

$$G_{nn'}(\Omega,\Omega') = \delta_{nn'}\rho^{(1)}(\Omega)\,\delta(\Omega|\Omega') - \rho^{(1)}(\Omega)\rho^{(1)}(\Omega') + (1-\delta_{nn'})\rho^{(2)}_{nn'}(\Omega,\Omega'). \tag{9}$$

$G_{nn'}(\Omega,\Omega')=G^{(s)}_{nn'}(\Omega,\Omega')+G^{(d)}_{nn'}(\Omega,\Omega')$ consists of a self-part and a distinct part, which are explicitly

$$G^{(s)}_{nn'}(\Omega,\Omega') = \delta_{nn'}[\rho^{(1)}(\Omega)\,\delta(\Omega|\Omega') - \rho^{(1)}(\Omega)\rho^{(1)}(\Omega')], \tag{10a}$$

$$G^{(d)}_{nn'}(\Omega,\Omega') = (1-\delta_{nn'})[\rho^{(2)}_{nn'}(\Omega,\Omega') - \rho^{(1)}(\Omega)\rho^{(1)}(\Omega')]. \tag{10b}$$

Due to the properties (6) and (7) of the particle distribution functions, $G_{nn'}(\Omega,\Omega')$ and $G^{(s)}_{nn'}(\Omega,\Omega')$ fulfill for all nn',

$$\int_{S^2} G_{nn'}(\Omega,\Omega')d\Omega = \int_{S^2} G_{nn'}(\Omega,\Omega')d\Omega' = 0, \tag{11a}$$

$$\int_{S^2} G^{(s)}_{nn'}(\Omega,\Omega')d\Omega = \int_{S^2} G^{(s)}_{nn'}(\Omega,\Omega')d\Omega' = 0. \tag{11b}$$

For the lattice system, the pair and total correlation functions $g_{nn'}(\Omega,\Omega')$ and $h_{nn'}(\Omega,\Omega')$ are introduced in the same manner as for a liquid [1,2],

$$g_{nn'}(\Omega,\Omega') = \frac{\rho^{(2)}_{nn'}(\Omega,\Omega')}{\rho^{(1)}(\Omega)\rho^{(1)}(\Omega')} \quad (n\neq n'), \tag{12}$$

$$h_{nn'}(\Omega,\Omega') = g_{nn'}(\Omega,\Omega') - 1 \quad (n\neq n'). \tag{13}$$

In contrast to Eq. (11), it is in general

$$\int_{S^2} h_{nn'}(\Omega,\Omega')d\Omega \neq 0, \int_{S^2} h_{nn'}(\Omega,\Omega')d\Omega' \neq 0 \quad (n\neq n'). \tag{14}$$

The same is true for $g_{nn'}(\Omega,\Omega')$. But, due to Eqs. (6), (7), (12), and (13),

$$\int_{S^2} \rho^{(1)}(\Omega)h_{nn'}(\Omega,\Omega')d\Omega = 0 \quad (n\neq n'), \tag{15a}$$

$$\int_{S^2} h_{nn'}(\Omega,\Omega')\rho^{(1)}(\Omega')d\Omega' = 0 \quad (n\neq n'). \tag{15b}$$

In the asymptotic limit of large particle separations, $g_{nn'}(\Omega,\Omega')$ and $h_{nn'}(\Omega,\Omega')$ in the disordered phase behave like

$$\lim_{|\mathbf{x}_{nn'}|\to\infty} g_{nn'}(\Omega,\Omega') = 1, \tag{16}$$

$$\lim_{|\mathbf{x}_{nn'}|\to\infty} h_{nn'}(\Omega,\Omega') = 0, \tag{17}$$

independent of the direction of $\mathbf{x}_{nn'}$. This follows due to $\lim_{|\mathbf{x}_{nn'}|\to\infty}\rho^{(2)}_{nn'}(\Omega,\Omega')\to\rho^{(1)}(\Omega)\rho^{(1)}(\Omega')$, which is in full agreement with the behavior of a liquid system.

The reader should note that it is the definition (12) and (13) of $g_{nn'}(\Omega,\Omega')$ and $h_{nn'}(\Omega,\Omega')$, respectively, which causes problems in case of hard potentials, because the denominator in Eq. (12) vanishes for orientations with Ω or Ω' in the sterically forbidden region $\overline{K}$ [see discussion in paragraph above Eq. (8)].

Making use of Eqs. (10), (12), and (13) and introducing

$$D(\Omega,\Omega') = 4\pi[\rho^{(1)}(\Omega)\delta(\Omega|\Omega') - \rho^{(1)}(\Omega)\rho^{(1)}(\Omega')] \tag{18}$$

we can rewrite $G^{(\alpha)}_{nn'}(\Omega,\Omega')$, $\alpha=s,d$, as follows:

$$G^{(s)}_{nn'}(\Omega,\Omega') = \frac{1}{4\pi}\delta_{nn'}D(\Omega,\Omega'), \tag{19a}$$

$$G^{(d)}_{nn'}(\Omega,\Omega') = (1-\delta_{nn'})\rho^{(1)}(\Omega)h_{nn'}(\Omega,\Omega')\rho^{(1)}(\Omega'). \tag{19b}$$

As for molecular liquids [2] (see also, e.g., Refs. [3,4,21,22]) we will expand all orientation-dependent functions with respect to spherical harmonics $Y_\lambda(\Omega)$, $\lambda=(lm)$. [1]Consequently, we have for any functions $f(\Omega)$ and $F_{nn'}(\Omega,\Omega')$ their λ transforms and the corresponding inverse transformations,

$$f_\lambda = i^l\int_{S^2} f(\Omega)Y_\lambda(\Omega)d\Omega, \tag{20a}$$

$$f(\Omega) = \sum_\lambda (-i)^l f_\lambda\, Y^*_\lambda(\Omega), \tag{20b}$$

$$F_{nn',\lambda\lambda'} = i^{l'-l}\int_{S^2}\int_{S^2} F_{nn'}(\Omega,\Omega')Y^*_\lambda(\Omega)Y_{\lambda'}(\Omega')d\Omega\, d\Omega', \tag{21a}$$

$$F_{nn'}(\Omega,\Omega') = \sum_{\lambda\lambda'}(-i)^{l'-l}F_{nn',\lambda\lambda'}\, Y_\lambda(\Omega)Y^*_{\lambda'}(\Omega'). \tag{21b}$$

The purely imaginary prefactors in Eqs. (20) and (21) are taken in agreement with Ref. [21].

Finally, we can use the lattice Fourier transform due to the lattice translational invariance. It is restricted to the first Brillouin zone (BZ) of volume V_{BZ}. For example, the transform of the site-site matrix elements (21a) and its inverse are given by

$$F_{\lambda\lambda'}(\mathbf{q}) = \sum_{\mathbf{x}_{nn'}} \mathrm{e}^{i\mathbf{q}\cdot\mathbf{x}_{nn'}}F_{nn',\lambda\lambda'}, \tag{22a}$$

$$F_{nn',\lambda\lambda'} = \frac{1}{V_{\mathrm{BZ}}}\int_{1\cdot\mathrm{BZ}} F_{\lambda\lambda'}(\mathbf{q})\mathrm{e}^{-i\mathbf{q}\cdot\mathbf{x}_{nn'}}d^3q. \tag{22b}$$

Symmetry properties of the one-particle distribution $\rho^{(1)}(\Omega)$ and of $G_{nn'}(\Omega,\Omega')$ and its λ transform are presented in Appendix A. These properties will be useful in the following.

[1]Instead, one could also use a complete set of functions, determined by the rotational symmetry. If $\mathcal{P}$ is the point symmetry group of the lattice and $\mathcal{P}_M$ the symmetry group of the molecules, one can use basis functions for irreducible representations of the symmetry group of $\rho^{(1)}(\Omega)$, which is a subgroup of $\mathcal{P}\otimes\mathcal{P}_M$ [8,13,14]. For axially symmetric particles, these are linear combinations of the spherical harmonics $Y_\lambda(\Omega),\lambda=(lm)$ [8,13].

III. ORNSTEIN-ZERNIKE EQUATION AND PERCUS-YEVICK APPROXIMATION

Similarly to simple and molecular liquids, we will introduce the direct correlation function $c_{nn'}(\Omega,\Omega')$, which is related to $h_{nn'}(\Omega,\Omega')$ by the OZ equation. Since $c_{nn'}(\Omega,\Omega')$ is determined by the inverse functions of $G^{(s)}_{nn'}(\Omega,\Omega')$ and $G_{nn'}(\Omega,\Omega')$, one has to be careful because of relations (11), which imply that a constant function $f(\Omega)=\mathrm{const}$ is an eigenfunction of $G^{(s)}_{nn'}(\Omega,\Omega')$ and $G_{nn'}(\Omega,\Omega')$ with eigenvalue zero. Therefore, these inverses do not exist on the one-dimensional subspace of constant functions. This feature is typical for molecular crystals.

However, the problem of inverting the (Ω,Ω')-dependent correlators can easily be solved by taking their λ transforming equation (21a). In addition, it is convenient to use the Fourier transformed quantities. Hence we will investigate matrices $\mathbf{G}(\mathbf{q})$ and $\mathbf{G}^{(s)}(\mathbf{q})$ with elements

$$G_{\lambda\lambda'}(\mathbf{q}) = \frac{1}{N}\langle\delta\rho^*_\lambda(\mathbf{q})\delta\rho_{\lambda'}(\mathbf{q})\rangle \equiv \frac{1}{4\pi}S_{\lambda\lambda'}(\mathbf{q}), \tag{23}$$

$$G^{(s)}_{\lambda\lambda'}(\mathbf{q}) = \frac{1}{4\pi}D_{\lambda\lambda'}, \tag{24}$$

which are zero for $l=0$ and/or $l'=0$ because of Eq. (11). However, $h_{\lambda\lambda'}(\mathbf{q})$, $g_{\lambda\lambda'}(\mathbf{q})$ in general [the same is true for the direct correlation function matrix elements $c_{\lambda\lambda'}(\mathbf{q})$ introduced in Eq. (33)] do not vanish for $l=0$ and/or $l'=0$. In order to avoid confusion it is convenient to use

$$F_{\lambda\lambda'} \equiv F^{\circ}_{\lambda\lambda'} \quad (l\geqslant 1, l'\geqslant 1). \tag{25}$$

If the first row and column of $\mathbf{F}$ vanish, its physical content is in $\mathbf{F}^\circ$, only. Since $\mathbf{G}$ and $\mathbf{G}^{(s)}=1/4\pi\,\mathbf{D}$ are of this form, inversion has to be done with respect to $\mathbf{G}^\circ$ and $\mathbf{D}^\circ$.

This behavior has also consequences in Ω space. In general, correlation functions $F(\Omega,\Omega')$, such as $h_{nn'}(\Omega,\Omega')$, will have "unphysical" parts, $\int\int F(\Omega,\Omega')d\Omega\, d\Omega'$, $\int F(\Omega,\Omega')d\Omega'$, and $\int F(\Omega,\Omega')d\Omega$. In that case their "physical" part is given by

$$F^\circ(\Omega,\Omega') = \int_{S^2}\int_{S^2} R(\Omega,\Omega'')F(\Omega'',\Omega''')R(\Omega''',\Omega')d\Omega''d\Omega''', \tag{26}$$

where the projector $R(\Omega,\Omega')=\delta(\Omega|\Omega')-1/4\pi$ projects out the unphysical parts. The reader should note that this is different to the decomposition of the pair potential into an isotropic part $\int\int v_{nn'}(\Omega,\Omega')d\Omega\, d\Omega'$ and crystal field terms related to $\int v_{nn'}(\Omega,\Omega')d\Omega$ and $\int v_{nn'}(\Omega,\Omega')d\Omega'$ [9–11]. In that case these terms have a physical meaning.

It is straightforward to prove that for the λ transform of $F^\circ(\Omega,\Omega')$ it is $F_{\lambda\lambda'}=0$ for $l=0$ and/or $l'=0$. This is reasonable since the λ transformings of the correlation functions

with $l=0$ and/or $l'=0$ do not describe orientational degrees of freedom and therefore are unphysical.

Using Eqs. (15) and (18) one gets

$$[\rho^{(1)}(\Omega)h(\Omega,\Omega',\mathbf{q})\rho^{(1)}(\Omega')]_{\lambda\lambda'} = \frac{1}{(4\pi)^2}\sum_{\lambda''\lambda'''(l''l'''\neq 0)} \overset{\circ}{D}_{\lambda\lambda''}\overset{\circ}{h}_{\lambda''\lambda'''}(\mathbf{q})\overset{\circ}{D}_{\lambda'''\lambda'}, \quad (27)$$

which implies

$$\mathbf{S}^{\circ}(\mathbf{q}) = \mathbf{D}^{\circ} + \frac{1}{4\pi}\mathbf{D}^{\circ}\,\mathbf{h}^{\circ}(\mathbf{q})\mathbf{D}^{\circ} \equiv 4\pi\,\mathbf{G}^{\circ}(\mathbf{q}). \quad (28)$$

Here, the Fourier transform $\mathbf{h}^{\circ}(\mathbf{q})$ has to be determined by using the constraint for all $\lambda\lambda'$,

$$\overset{\circ}{h}_{nn,\lambda\lambda'} = 0. \quad (29)$$

Equation (28) generalizes the well-known relation between the static correlator $S(q)$ and the total correlation function $h(q)$ for liquids [cf. Eq. (1)] to molecular crystals.

Now we are in a position to introduce the direct correlation function $\mathbf{c}^{\circ}(\mathbf{q})$ and to derive the OZ equation. $\mathbf{c}^{\circ}(\mathbf{q})$ is defined by

$$\mathbf{c}^{\circ}(\mathbf{q}) = (\mathbf{G}^{(s)\circ})^{-1} - (\mathbf{G}^{\circ}(\mathbf{q}))^{-1}. \quad (30)$$

Substituting $(\mathbf{G}^{\circ}(\mathbf{q}))^{-1}$ from Eq. (30) and $\mathbf{G}^{\circ}(\mathbf{q})$ from Eq. (28) into

$$(\mathbf{G}^{\circ}(\mathbf{q}))^{-1}\,\mathbf{G}^{\circ}(\mathbf{q}) = \mathbf{1}^{\circ}$$

and making use of Eq. (19a) yields the OZ equation

$$\mathbf{h}^{\circ}(\mathbf{q}) = \mathbf{c}^{\circ}(\mathbf{q}) + \frac{1}{4\pi}\mathbf{c}^{\circ}(\mathbf{q})\mathbf{D}^{\circ}\,\mathbf{h}^{\circ}(\mathbf{q}). \quad (31)$$

The back transformation of Eq. (31) leads to the OZ equation in real and angular spaces,

$$(1-\delta_{nn'})\overset{\circ}{h}_{nn'}(\Omega,\Omega') = \overset{\circ}{c}_{nn'}(\Omega,\Omega') + \frac{1}{4\pi}\sum_{n''(\neq n')}\int_{S^2}\int_{S^2} \times \overset{\circ}{c}_{nn''}(\Omega,\Omega'')D^{\circ}(\Omega'',\Omega''') \times \overset{\circ}{h}_{n''n'}(\Omega''',\Omega')d\Omega''\,d\Omega'''. \quad (32)$$

Note that $\overset{\circ}{c}_{nn}(\Omega,\Omega')\neq 0$, in general.

This result is almost the same as for molecular liquids [2]. There are two main differences. First, we have to use all matrices with the first row and column of the original matrices skipped. Second, there appears the matrix $\mathbf{D}^{\circ}$ and third the Fourier backtransform of $\mathbf{h}^{\circ}(\mathbf{q})$ has to fulfill the condition (29) for all $\lambda\lambda'$.

Up to now, the equations are not closed. Since neither the total correlation nor the direct correlation function is given, the previous concepts are almost useless if one is interested in an analytical approach to determine the structure factors (23) and (28). An additional equation, called the closure relation, must be used to find a self-consistent solution for $\mathbf{h}(\mathbf{q})$ and $\mathbf{c}(\mathbf{q})$, as for simple and molecular liquids. It has been our intention to follow as close as possible the established lines of liquid theory, and so we chose the most straightforward analogon of the PY approximation for the lattice, which is for $n\neq n'$,

$$c_{nn'}(\Omega,\Omega') = f_{nn'}(\Omega,\Omega')(g_{nn'}(\Omega,\Omega') - c_{nn'}(\Omega,\Omega')) = f_{nn'}(\Omega,\Omega')(1 + h_{nn'}(\Omega,\Omega') - c_{nn'}(\Omega,\Omega')). \quad (33)$$

Note that Eq. (32) involves $\overset{\circ}{c}_{nn'}(\Omega,\Omega')$ and $\overset{\circ}{h}_{nn'}(\Omega,\Omega')$, only, but in Eq. (33) the full functions $c_{nn'}(\Omega,\Omega')$ and $h_{nn'}(\Omega,\Omega')$ appear. It can be shown for hard particles and $n\neq n'$ that $\overset{\circ}{c}_{nn'}(\Omega,\Omega')$ already determines $c_{nn'}(\Omega,\Omega')$ uniquely [20], and the same is true for $\overset{\circ}{h}_{nn'}(\Omega,\Omega')$ and $h_{nn'}(\Omega,\Omega')$ [see Appendix B, Eq. (B7)]. $f_{nn'}(\Omega,\Omega')$ is the Mayer f function, which is

$$f_{nn'}(\Omega,\Omega') = \exp\{-\beta V_{nn'}(\Omega_n,\Omega_{n'})\} - 1 \quad (34)$$

for $n\neq n'$. For hard particles, the pair potential is $V_{nn'}(\Omega,\Omega')=0$ [if the pair $(n\Omega,n'\Omega')$ has no overlap] and $V_{nn'}(\Omega,\Omega')=\infty$ (if the pair has overlap). This implies

$$f_{nn'}(\Omega,\Omega') = \begin{cases} 0, & \text{no overlap} \\ -1, & \text{overlap.} \end{cases} \quad (35)$$

The range of the f function for hard ellipsoids is $\max(a,b)$, if the ellipsoids are fixed with their centers of mass on the lattice. In accordance with the theory of liquids of hard particles, Eq. (33) yields $g_{nn'}(\Omega,\Omega')=0 \leftrightarrow \rho^{(2)}_{nn'}(\Omega,\Omega')=0$, while $c_{nn'}(\Omega,\Omega')$ remains undetermined, if $(n\Omega,n'\Omega')$ has overlap and $c_{nn'}(\Omega,\Omega')=0$ while $g_{nn'}(\Omega,\Omega')$ remains undetermined, if $(n\Omega,n'\Omega')$ has no overlap [1,2].

The λ transform of the Mayer function will be nonzero for $l=0$ and/or $l'=0$. The same holds for the λ transforming of $c_{nn'}(\Omega,\Omega')$. Therefore the direct and, as stressed above, the total correlation function related by the PY approximation contain unphysical parts, in contrast to the direct and total correlation functions related by the OZ equation. Fortunately, this will not introduce a serious problem as will be discussed in Sec. IV B and shown in more detail in Appendixes B and C, and in Ref. [20].

IV. RESULTS FOR HARD ELLIPSOIDS ON A SIMPLE CUBIC LATTICE

The self-consistent solution of the OZ equation and the PY approximation has been done numerically. In order to check the quality of these solutions we have performed MC simulations, which also allow to determine the phase boundary between orientationally ordered and disordered phases. We stress that the investigation of the phase transition has not been our major motivation. Therefore we have not attempted to verify the phase boundary by more sophisticated MC algorithms. Before we describe the numerical solution of the OZ/PY equations in Sec. IV B, let us present some details of the MC simulations in the following section. The results from both approaches will be discussed in Sec. IV C.

For both, the numerical solution of the OZ equation using the PY approximation and the MC studies the overlap crite-

rion of Vieillard-Baron [23] for hard ellipsoids of revolution is used.

A. MC simulations

The MC simulations are performed for a simple cubic lattice with $16\times16\times16$ sites and periodic boundary conditions. For systems having very long-ranged correlations along a certain lattice direction, test runs with $32\times32\times32$ particles are done, but the results are only slightly different and not shown in this work.

The only possible MC move is a rotation for a randomly chosen particle perpendicularly to its orientation axis $\mathbf{u}_n$ by an angle $0\leqslant\theta\leqslant\theta_{\max}\leqslant\pi$, where $\cos\theta$ is at random, and a subsequent rotation with respect to its original orientation by a random angle $0\leqslant\phi\leqslant2\pi$. If this move leads not to an overlap of ellipsoids, it is accepted, otherwise rejected, in which case the next move is not tried for the same particle, but for a new randomly chosen one.

As starting configuration for each MC run parallel ellipsoids are chosen. Each particle is moved on an average of 1000 times with $\theta_{\max}=\pi/2$ to get a rapid convergence to the disordered phase having a cubic symmetry, if possible. Afterwards, $\theta_{\max}$ is adjusted to an acceptance rate of 25% and the system is equilibrated well before the production phase.

To discriminate between the disordered and ordered phases, we have used several criteria [20]. Let us describe two of them. First, after equilibration we have calculated the largest eigenvalue λ_+ of the Saupe tensor [24] for a given size of the lattice. Note that λ_+ is related to $\langle Y_{2m}\rangle$, $m=-2,\ldots,2$, and that $\lambda_+\geqslant0$. Due to finite size effects λ_+ becomes small, but nonzero in the disordered phase. We have checked that this small value decreases with increasing system size, as it should be in the disordered phase. Second, the symmetry relations, Eq. (A3), which hold in the disordered phase only, were used. For instance, calculating $\langle Y_{4\pm4}\rangle$ and $\langle Y_{40}\rangle$ from the MC trajectories the ratio $\langle Y_{4\pm4}\rangle/\langle Y_{40}\rangle$ should be close to the exact value $\frac{1}{14}\sqrt{70}$ [cf. Eq. (A3)]. Since this test involves $l\geqslant2$, it is more reliable, because one cannot exclude that an orientational order exists for which $\langle Y_{2m}\rangle=0$.

The resulting phase diagrams for prolate and oblate ellipsoids are shown in Fig. 2. The thin solid lines characterize the closest packing of parallel ellipsoids. They represent upper bounds for the phase boundaries for transitions to ordered phases with *aligned* ellipsoids. Whether there exist more complex ordered phases, commensurate, or incommensurate ones with even larger volume fraction than on the thin solid lines is not known. An interesting feature of these lines can be observed. For prolate and oblate ellipsoids there are characteristic pairs (a,b) at which cusps occur, indicating a maximum volume fraction. The light gray areas represent the transition region from an orientationally disordered to an ordered phase. The latter is not necessarily a phase of aligned ellipsoids. Transitions have been observed from the ordered to the disordered phases and also vice versa for systems with ellipsoids of small enough maximum linear dimension, having only few interaction partners. The hysteresis is small, indicating either a continuous or a weakly first-order phase

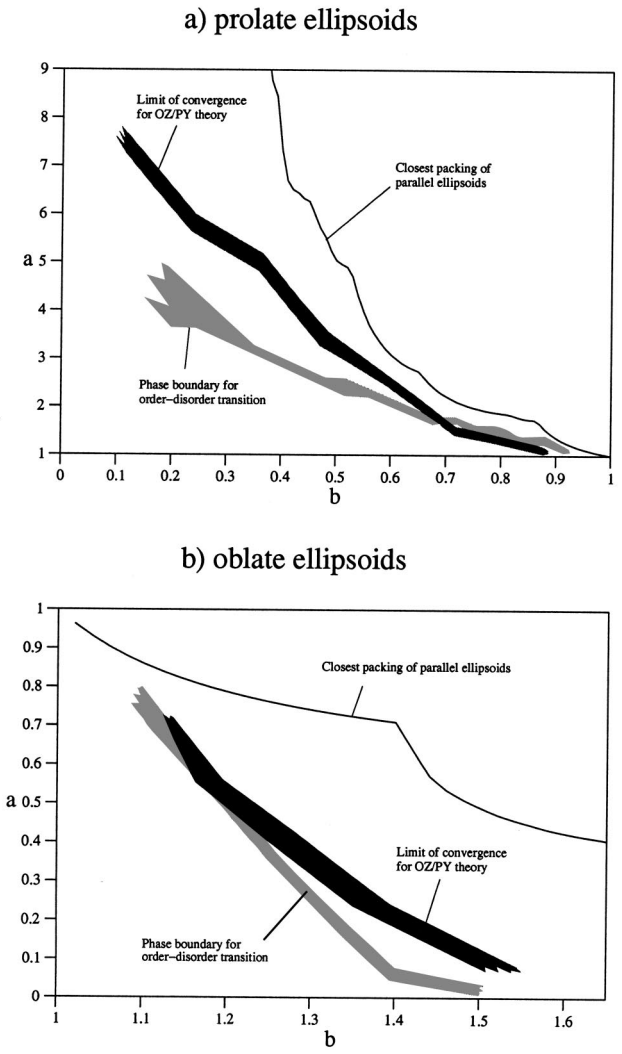

FIG. 2. Phase diagrams for (a) prolate and (b) oblate hard ellipsoids of revolution on a simple cubic lattice. Solid lines refer to the closest packing for parallel ellipsoids. Within the light gray areas an order-disorder phase transition occurs, while the dark gray areas indicate where the numerical solution of the OZ/PY equations starts to diverge. For a more detailed discussion see text of Secs. IV A and IV B. In the figures above, areas are used instead of error bars.

transition. The dark gray areas refer to the OZ/PY solution and indicate where the iteration scheme described in Sec. IV B and Appendix C turns from convergent to divergent.

B. Numerical solution of the OZ equation using the PY approximation

The numerical solution of the OZ/PY equations is performed by the iterative procedure described in Appendix C for lattices of size $32\times32\times32$ and periodic boundary conditions. The head-tail symmetry of the particles restricts the number of nonzero matrix elements for $\mathbf{G}_{nn'}$, $\mathbf{c}_{nn'}$ (and $\mathbf{h}_{nn'}$, $\mathbf{f}_{nn'}$ for $n\neq n'$) to l and l' even. The only exception is the self-part of $\mathbf{G}_{nn'}$ (see Appendix A). The numerical solution of the OZ/PY equations requires a truncation of these matri-

ces at $l_{\max}$, with exception of $\mathbf{f}_{nn'}$ which is cut at $2\,l_{\max}$. Usually we have chosen $l_{\max}=4$. For some systems, characterized by (a,b), we have also taken $l_{\max}=2$ and $l_{\max}=6$. All the correlators we have investigated remain qualitatively unchanged, while the correlation lengths of these correlators become larger for increasing $l_{\max}$. For those systems showing no convergence of the iteration scheme because of diverging correlation lengths for $l_{\max}=4$ and $32\times32\times32$ lattice sites, system sizes up to $128\times128\times128$ have been used. But then also for none of these bigger system sizes convergence could be achieved.

For the iteration procedure it is convenient to use the λ-transform of the PY equation (33),

$$c_{nn',\lambda\lambda'} = \sum_{\lambda_1\lambda_2\lambda_3\lambda_4} A(\lambda\lambda'|\lambda_1\lambda_2,\lambda_3\lambda_4) f_{nn',\lambda_1\lambda_2} \times (g_{nn',\lambda_3\lambda_4} - c_{nn',\lambda_3\lambda_4}), \tag{36}$$

where

$$A(\lambda\lambda'|\lambda_1\lambda_2,\lambda_3\lambda_4) = i^{l'-l+l_1-l_2+l_3-l_4}\left[\frac{(2l_1+1)(2l_3+1)}{4\pi(2l+1)}\right]^{1/2} \times\left[\frac{(2l_2+1)(2l_4+1)}{4\pi(2l'+1)}\right]^{1/2} C(l_1l_3l,000) \times C(l_2l_4l',000)C(l_1l_3l,m_1m_3m) \times C(l_2l_4l',m_2m_4m') \tag{37}$$

with $C(l_1l_2l_3,m_1m_2m_3)$ the Clebsch-Gordon coefficients [2].

The self-consistent solution of the OZ/PY equations needs $\overset{\circ}{D}_{\lambda\lambda'}$ and $f_{nn',\lambda\lambda'}$ as input, which will be given in Appendix B. Convergence of the iteration is assumed after the relative change of the correlators has submerged a certain threshold. Then the fix point solution $\mathbf{h}^\circ(\mathbf{q})$ is taken to calculate $\mathbf{S}(\mathbf{q})$ from Eq. (28) and $\mathbf{G}_{nn'}$ by back transformation.

C. Numerical results for the correlation functions

Results obtained from the numerical solution of the OZ/PY equations and the MC simulations are presented in Figs. 3–8 for four different pairs of (a,b), including prolate and oblate ellipsoids. We have restricted the illustrations of correlators in direct and reciprocal space to the matrix elements $(l=l'=2,m=m'=0,1,2)$, $(l=2,l'=4,m=m'=0,1,2)$, and $(l=l'=4,m=m'=0,1,2,3,4)$.

Log-lin representations of the direct space orientational correlators $G_{n0,\lambda\lambda'}$ are shown along lattice directions of high symmetry, i.e., $\mathbf{x}_{n0}=(0,0,n)$, $(0,n,n)$, and (n,n,n) for $n=0,1,\cdots,8$ [part (a) of Figs. 3–8]. Along these directions, all $G_{n0,\lambda\lambda'}$ are real for the chosen $\lambda\lambda'$, by the symmetries (A5). Note that a step $\Delta n=1$ corresponds to different lengths in direct space, namely 1, $\sqrt{2}$, and $\sqrt{3}$ for the different lattice directions. For each $m=m'$ and each lattice direction, a separate picture is provided and a logarithmic plotting has been chosen for positive and negative values of $G_{n0,\lambda\lambda'}$ separately, i.e., the negative values are presented as $-\ln|G_{n0,\lambda\lambda'}|$. This plotting shows that the direct space correlations decay exponentially in most cases. The respective values of $\mathbf{x}_{n0}$ and $\lambda\lambda'$ are included, too. Note that the scatter of the MC data for some $\lambda\lambda'$ and larger values of n is due to the error margins.

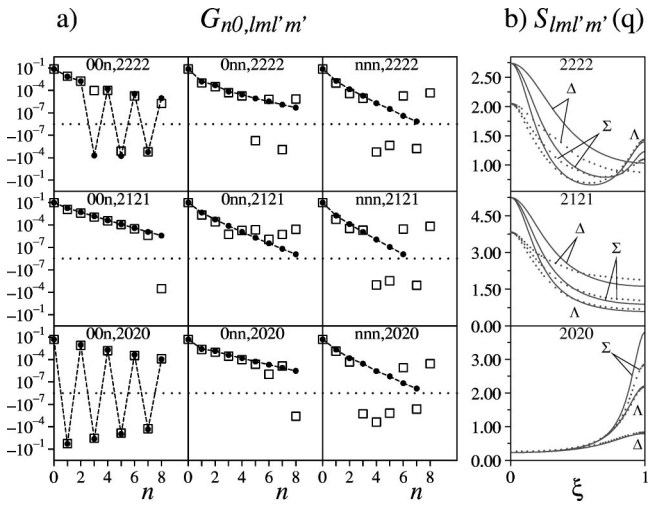

FIG. 3. (a) Log-lin representation of the direct space orientational correlators $G_{n0,2m2m}$ along highly symmetric lattice directions (solid circles = OZ/PY results, squares = MC results; dashed lines are a guide to the eye), (b) orientational structure factors $S_{2m2m}(\mathbf{q})$ along the respective reciprocal lattice directions (solid lines =OZ/PY results, dotted lines=MC results). These results are for oblate hard ellipsoids with axes $a=0.4$, $b=1.2$ on a simple cubic lattice with lattice constant equal to one and $m=0,1,2$. For further explanation see text of Sec. IV C.

Similarly to direct space, only correlators $S_{\lambda\lambda'}(\mathbf{q})$ along highly symmetric reciprocal lattice directions are displayed, i.e., $\mathbf{q}=\xi(0,0,\pi)$, $\xi(0,\pi,\pi)$, and $\xi(\pi,\pi,\pi)$ for $0\leqslant\xi\leqslant1$, which are the correlators from the Brillouin zone center to its edge in the respective direction [part (b) of Figs. 3–8]. The curves are distinguished by the symbols Δ **(**$(0,0,\pi)$ direction**)**, Σ **(**$(0,\pi,\pi)$ direction**)**, and Λ **(**(π,π,π) direction**)**, as usual in solid state physics. All $S_{\lambda\lambda'}(\mathbf{q})$ which are shown are real by the symmetries (A6). Additionally, by Eq. (23), the diagonal elements $S_{2m2m}(\mathbf{q})$ and $S_{4m4m}(\mathbf{q})$ are positive. The numerically determined correlators $S_{\lambda\lambda'}(\mathbf{q})$ have been interpolated by cubic splines with the correct

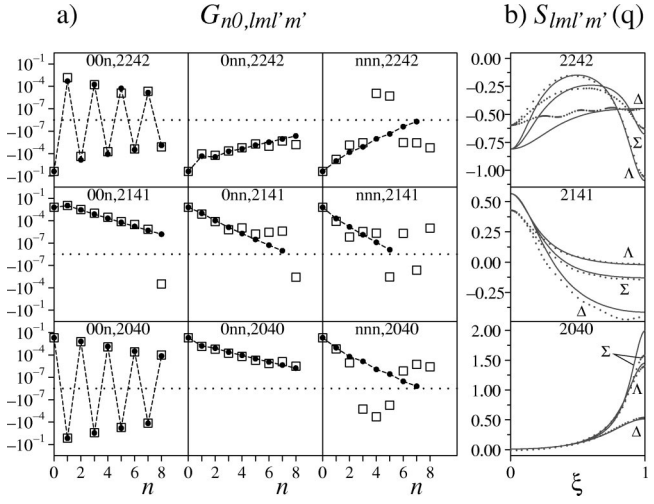

FIG. 4. Same as in Fig. 3, but for $l=2$, $l'=4$.

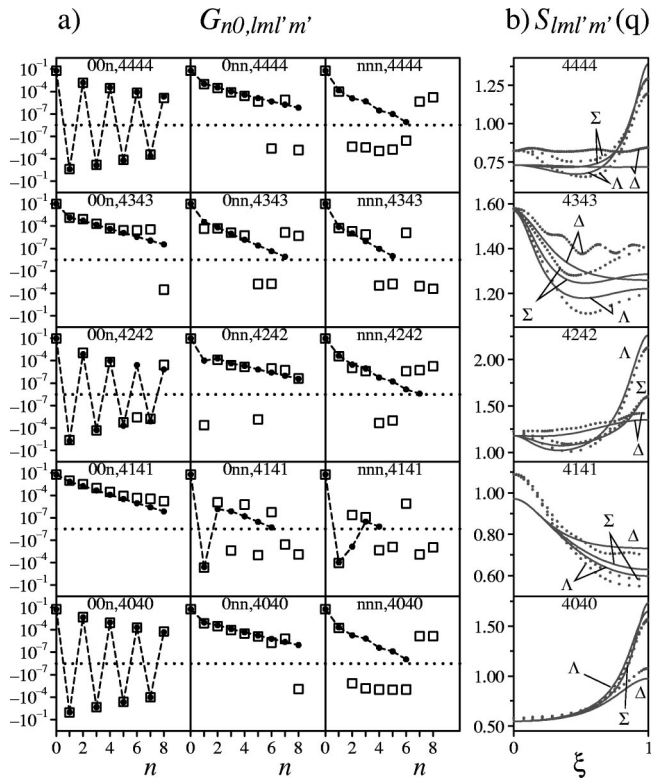

FIG. 5. Same as in Fig. 3, but for $l=l'=4$ and $m=0,1,2,3,4$.

boundary condition of vanishing gradients for $\xi=0$ and $\xi=1$. Note the different scales of the illustrations for different $\lambda\lambda'$.

Let us first start by discussing the results for *oblate* hard ellipsoids with axes $a=0.4$ and $b=1.2$ shown in Figs. 3–5. This system has a packing fraction of $\phi\approx 0.3$ and is quite close to the MC phase boundary shown in Fig. 2(b), but not close enough to find a tendency to a divergence of some of the $S_{\lambda\lambda'}(\mathbf{q})$. Notice the almost perfect agreement of the OZ/PY and MC orientational correlators in direct

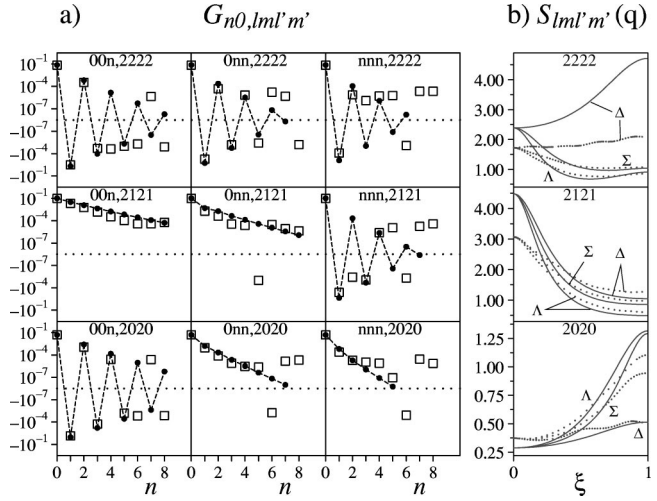

FIG. 6. Same as in Fig. 3, but for prolate hard ellipsoids with axes $a=1.6$, $b=0.6$.

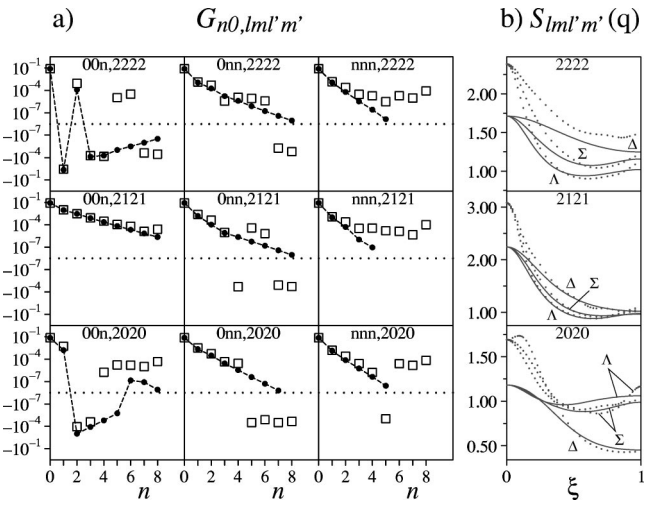

FIG. 7. Same as in Fig. 3, but for prolate hard ellipsoids with axes $a=3.6$, $b=0.24$.

space, in case where the MC results are large enough. In fact, such an agreement appears for all investigated oblate ellipsoid systems, for which MC results are available, except for the system with $a=0.72$, $b=1.1$. Relatively long-ranged oscillations appear for all correlators along the fourfold lattice direction $[0,0,1]$ having *even* $m=m'$. The other correlators along the same direction decay faster and monotonously without oscillation, and also the correlators along the other directions decay without oscillations. Note that for $a=0.4$ and $b=1.2$ the ellipsoids can only interact via their nearest neighbors, which are localized along the fourfold lattice directions. Therefore, it is tempting to assume that the oscillations are primarily related to a direct particle interaction via nearest neighbors along a certain lattice direction. For denser oblate and some prolate systems, the oscillations extend up to many lattice constants. For the structure factors $S_{\lambda\lambda'}(\mathbf{q})$, the agreement of OZ/PY and MC results is satisfactory. The most significant deviations appear for $l=l'=2$ near $\mathbf{q}=\mathbf{0}$. The oscillations exhibited by some of the $G_{n0,\lambda\lambda'}$ manifest them-

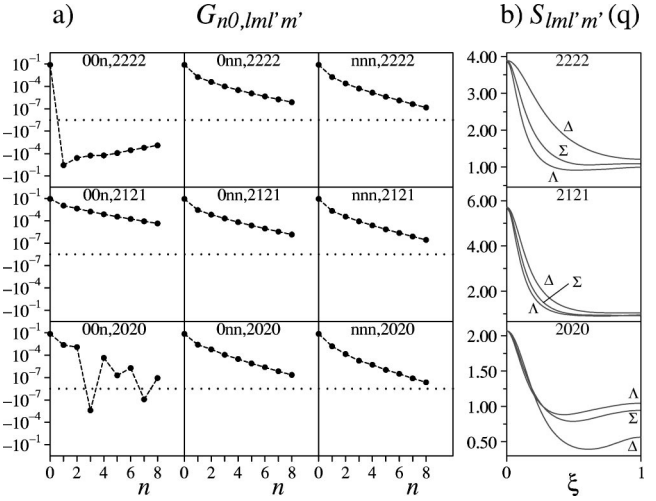

FIG. 8. Same as in Fig. 3, but for prolate hard ellipsoids with axes $a=4.8$, $b=0.24$.

selves in some maxima at the Brillouin zone edge, mainly for correlators $S_{2m2m}(\mathbf{q})$ and $S_{4m4m}(\mathbf{q})$ with m even, but also for the correlators $S_{2040}(\mathbf{q})$. Increasing a and/or b for oblate systems, the OZ/PY results for some of these zone-edge maxima show a tendency to diverge, accompanied by a simultaneous divergence mainly of the remaining $l=l'=2$ correlators at the zone center.

Now, we turn to *prolate* ellipsoids. Compared to oblate ellipsoids, the correlators for the prolate ones depend more sensitively on a and b. We show results for $l=l'=2$ only. Correlators with $(l,l')\neq(2,2)$, which were also calculated, do not yield new insight. First, we have chosen prolate ellipsoids with $a=1.6$, $b=0.6$, having a packing fraction of $\phi\approx 0.3$, for which some results are shown in Fig. 6. For this system, oscillations appear additionally along the two other lattice directions (i.e., $[0,1,1]$ and $[1,1,1]$), which confirm the assumption that they may be caused by direct interaction via nearest neighbors for appropriate values of b and not too large a. Again, the MC results in direct space match the analytical results very well, though latter overestimate some of the correlation lengths. The much too large OZ/PY results for the correlators $S_{2222}(\mathbf{q})$ at the zone boundary along the Δ direction are perhaps also due to this overestimation.

Now we pass to more and more elongated prolate ellipsoids and investigate what happens. In the limit of this process one obtains the hard-needle system, which is discussed, e.g., in Ref. [25]. Ellipsoids with axes $a=3.6$ and $b=0.24$ have a huge aspect ratio of $X_0=a/b=15$. Of course, the packing fraction of these ellipsoids on the simple cubic lattice is quite low, about 10%, but the frustration effect of the rigid lattice may provide completely new effects in comparison to a liquid. As shown in Fig. 7, the behavior of most of the correlators $G_{n0,2m2m}$ is rather monotonous in comparison to $a=1.6$ and $b=0.6$. Oscillations have disappeared completely, except some oscillatory transient behavior for the [0,0,1] direction and $\lambda=\lambda'=(22)$. However, $G_{n0,\lambda\lambda'}$ shows less regular variation along the [0,0,1] direction for $\lambda=\lambda'=(20)$. The OZ/PY results clearly underestimate the $S_{2m2m}(\mathbf{q})$ correlators for small $\mathbf{q}$. This is also the case for the $S_{2m2m}(\mathbf{q})$ correlators of other investigated systems in the neighborhood of $a=3.6$, $b=0.24$.

The last system we present consists of ellipsoids with $a=4.8$ and $b=0.24$, for which it is $X_0=20$ and $\phi\approx 16\%$. Results are shown in Fig. 8. The correlators in direct space essentially show monotonous decay, and the correlation lengths have clearly increased in comparison to $a=3.6$ and $b=0.24$. Unfortunately, this system lies beyond the MC phase boundary [see Fig. 2(a)], so that no MC results are available. Despite of the monotonous behavior of most correlators, the $G_{n0,2020}$ correlators along the [0,0,1] direction, for example, show irregular behavior, as it was the case for $a=3.6$ and $b=0.24$ (see Fig. 7). In Fig. 8, the beginning of a divergence of the $S_{2121}(\mathbf{q}=\mathbf{0})$ correlator is seen. The corresponding value for $a=5.6, b=0.24$ is about 20.

V. DISCUSSION AND CONCLUSIONS

Our main goal has been the study of static orientational correlation functions for a molecular crystal in its disordered phase. For this, we have derived the OZ equation, well known in liquid theory, for a rigid periodic lattice with internal orientational degrees of freedom. As a closure relation we have adopted the PY approximation. As pointed out, there are differences for the present approach to that for liquids. One of them is the fact that the OZ equation only involves the physical parts of the direct and total correlation functions, i.e., $c^{\circ}_{nn'}(\Omega,\Omega')$ and $h^{\circ}_{nn'}(\Omega,\Omega')$, whereas the PY approximation relates $c_{nn'}(\Omega,\Omega')$ and $h_{nn'}(\Omega,\Omega')$. Another important, well-known difference is the one-particle orientational distribution function $\rho^{(1)}(\Omega)$. In the isotropic phase of a molecular liquid it is $\rho^{(1)}(\Omega)=1/4\pi$, but due to the anisotropy of a crystal $\rho^{(1)}(\Omega)$ exhibits a nontrivial Ω dependence. In order to solve the OZ/PY equations, one has to calculate $\rho^{(1)}(\Omega)$ separately. In our case, we have performed MC simulations. Analytical approaches are also possible, e.g., for fixed a one could perform a kind of virial expansion for small b.

Despite these differences, the form of the OZ equation for a molecular crystal is quite similar to that for molecular liquids [2]. In order to explore the applicability of the lattice OZ equation in combination with the PY approximation, we have solved these equations for hard ellipsoids of revolution on a simple cubic lattice. Due to the orientational degrees of freedom, the orientational correlators $G_{nn',\lambda\lambda'}$ in direct space or $S_{\lambda\lambda'}(\mathbf{q})$ in reciprocal space, with $\lambda=(lm)$, are tensorial quantities. Accordingly, the self-consistent numerical solution of the OZ/PY equations requires a truncation at $l_{\max}$. We mainly have chosen $l_{\max}=4$. As a result, we have found orientational correlators which have less structure in direct and reciprocal spaces than for liquid systems. Nevertheless, there are some interesting features depending on the length a and b of the ellipsoid axes. For oblate ellipsoids and prolate ones of large enough b, some of the direct space orientational correlators exhibit oscillations in certain lattice directions. Since the oscillations have period two they lead to maxima of $S_{\lambda\lambda'}(\mathbf{q})$ at the Brillouin zone edge for some $\lambda\lambda'$. Although no long-range orientational order exists, the oscillatory behavior originates from an alternating reordering of the ellipsoids on a finite length scale, which can extend up to many lattice constants.

Decreasing for prolate ellipsoids b and increasing a leads to a disappearance of almost all of these significant oscillations. In this case, the correlators $S_{2m2m}(\mathbf{q})$ take their absolute maxima at the Brillouin zone center (cf. Figs. 7 and 8), indicating ferrorotational fluctuations, while this behavior is not found to the same extent for the other correlators (see also Ref. [20]). The behavior of the correlators $S_{2m2m}(\mathbf{q})$ resembles that of a liquid of ellipsoids with aspect ratio larger than about two which forms a nematic phase [26]. Surprisingly, increasing a for fixed b more and more the OZ/PY results for $S_{2m2m}(\mathbf{q})$ lead to a divergence at $\mathbf{q}=\mathbf{0}$, which indicates the tendency to establish a long-range ferrorotational order. This finding demonstrates that PY theory applied to *molecular crystals* can yield the onset of a phase transition to an ordered phase, as it was already found before for a liquid of hard ellipsoids [4].

Some correlators for appropriately long prolate ellipsoids exhibit rather irregular behavior in direct space, which is

nevertheless consistent with MC results (where available) and therefore has to be taken seriously (cf. Fig. 7). We suppose the frustration effect of the lattice to be the reason for this irregular behavior.

Comparison of the PY results with those from MC simulations shows a satisfactory agreement. But the quality of this agreement is less good than it is, e.g., for a liquid of hard spheres. The reason for this may lie in the PY approximation. For a liquid its physical content has been elucidated by Percus [27] (see also Ref. [1]) by use of a grand canonical ensemble. Since in a molecular crystal the particles are fixed, it is not obvious how this reasoning can be used. Of course, it might be interesting to investigate whether other closure relations [1] or the turn to much higher $l_{\max}$ can lead to an improvement.

To conclude, we have presented for molecular crystals a theoretical framework for the calculation of correlation functions. This has been achieved by an extension of the OZ equation from liquids to crystals. In combination with the PY approximation we have demonstrated that this framework leads to satisfactory results compared with MC data.

ACKNOWLEDGMENTS

We gratefully acknowledge helpful discussions and the support in performing the MC simulations by J. Horbach, M. Müller, and W. Paul.

APPENDIX A: SYMMETRY RELATIONS FOR THE ONE-PARTICLE DISTRIBUTION AND THE CORRELATION FUNCTIONS

In this appendix we will present some useful properties of the one-particle and two-particle quantities.

Let us first discuss the one-particle orientational distribution function $\rho^{(1)}(\Omega)$ in the disordered phase. $\rho^{(1)}(\Omega)$ must carry the full point symmetry $\mathcal{P}$ of the underlying periodic lattice, and also the symmetry $\mathcal{P}_M$ of the particles [8,13]. Neglecting the latter for a moment, $\rho^{(1)}(\Omega)$ for axially symmetric particles can be expanded into a series of all $\mathcal{P}$ invariant combinations $\hat{Y}_{ln_l}(\Omega)$ of spherical harmonics. This expansion reads [cf. (20b)]

$$\rho^{(1)}(\Omega) = \sum_{ln_l} (-i)^l \, \rho^{(1)}_{ln_l} \, \hat{Y}^*_{ln_l}(\Omega). \tag{A1}$$

Here, the numbers n_l are the multiplicities of the unity irreducible representation contained in the point group representation of $\mathcal{P}$ established by all spherical harmonics of order l. Then, by the invariance requirement under symmetry operations of the particles, Eq. (A1) can eventually be further simplified [8,13]. If the lattice is cubic, $\mathcal{P}=O_h$, and for any kind of axially symmetric particles we have

$$\rho^{(1)}(\Omega) = \frac{1}{\sqrt{4\pi}}\hat{Y}_{01}(\Omega) + \rho^{(1)}_{41} \, \hat{Y}_{41}(\Omega) - \rho^{(1)}_{61} \, \hat{Y}_{61}(\Omega) + \rho^{(1)}_{81} \, \hat{Y}_{81}(\Omega) + O(l=10). \tag{A2}$$

The O_h cubic invariants $\hat{Y}_{01}(\Omega)=Y_{00}(\Omega)=(4\pi)^{-1/2}$, $\hat{Y}_{41}(\Omega)$, $\hat{Y}_{61}(\Omega)$, and $\hat{Y}_{81}(\Omega)$ are *real* functions and given in Ref. [28] up to factors $(4\pi)^{-1/2}\rho^{-l}$. [2]In Sec. IV B and Appendix B, the canonical averages $\langle Y_\lambda\rangle = \int_{S^2} \rho^{(1)}(\Omega) Y_\lambda(\Omega) d\Omega$ are needed. The values $\langle\hat{Y}_{41}\rangle$, $\langle\hat{Y}_{61}\rangle$, and $\langle\hat{Y}_{81}\rangle$ have been calculated by MC simulations (see Sec. IV A) for several values of a and b. The nonvanishing $\langle Y_\lambda\rangle$ in the disordered phase up to $l=9$ are given by

$$\langle Y_{00}\rangle = \frac{1}{\sqrt{4\pi}}, \quad \langle Y_{40}\rangle = \frac{\sqrt{21}}{6}\langle\hat{Y}_{41}\rangle,$$

$$\langle Y_{4\pm4}\rangle = \frac{\sqrt{30}}{12}\langle\hat{Y}_{41}\rangle, \quad \langle Y_{60}\rangle = \frac{\sqrt{2}}{4}\langle\hat{Y}_{61}\rangle,$$

$$\langle Y_{6\pm4}\rangle = -\frac{\sqrt{7}}{4}\langle\hat{Y}_{61}\rangle, \quad \langle Y_{80}\rangle = \frac{\sqrt{33}}{8}\langle\hat{Y}_{81}\rangle,$$

$$\langle Y_{8\pm4}\rangle = \frac{\sqrt{42}}{24}\langle\hat{Y}_{81}\rangle, \quad \langle Y_{8\pm8}\rangle = \frac{\sqrt{390}}{48}\langle\hat{Y}_{81}\rangle. \tag{A3}$$

These relations also allow to check whether the system is in the disordered phase. For instance, calculating $\langle Y_{40}\rangle$ and $\langle Y_{4\pm4}\rangle$ from the MC trajectories, their ratio $\langle Y_{4\pm4}\rangle/\langle Y_{40}\rangle$ must be $\approx\frac{1}{14}\sqrt{70}$.

Next, we investigate the symmetries of $G_{nn'}(\Omega,\Omega')$, which will help to reduce the numerical effort to solve the OZ/PY equations. From definition (8) it follows immediately

$$G_{nn'}(\Omega,\Omega') = G_{n'n}(\Omega',\Omega). \tag{A4a}$$

If the inversion I belongs to $\mathcal{P}$, the inverted $G_{nn'}(\Omega,\Omega')$ must match the old one by use of Eq. (8), since $H(\{\Omega_n\},\{\mathbf{l}_n\})$ remains unchanged under inversion then

$$G_{n'n}(-\Omega,-\Omega') = G_{nn'}(\Omega,\Omega'), \tag{A4b}$$

where $\Omega=(\theta,\phi)\leftrightarrow-\Omega\equiv I\Omega=(\pi-\theta,\phi+\pi)$ has been used. If the symmetry group $\mathcal{P}$ contains rotations R, the rotated $G_{nn'}(\Omega,\Omega')$ must be the original one,

$$G_{Rnn'}(R\Omega,R\Omega') = G_{nn'}(\Omega,\Omega'), \tag{A4c}$$

where Rnn' stands for $R\mathbf{x}_{nn'}$. The properties (A4a)–(A4c) yield for $G_{nn',\lambda\lambda'}$,

$$G_{nn',\lambda\lambda'} = G^*_{n'n,\lambda'\lambda}, \tag{A5a}$$

$$G_{nn',\lambda\lambda'} = (-1)^{l+l'} G_{n'n,\lambda\lambda'}, \tag{A5b}$$

[2]In our opinion, the factor $\frac{1}{6}$ in the expression for α_8 in Ref. [28] is a misprint and should read $\frac{1}{3}$ instead.

$$G_{Rnn',lm,l'm'} = \sum_{m''m'''} D^{l}_{mm''}(R) D^{l'^{*}}_{m'm'''}(R) G_{nn',lm'',l'm'''}. \tag{A5c}$$

In Eq. (A5c), Wigner's generalized spherical harmonics (rotation matrices) are used [2]. The reader should note that for the calculation of the correct rotation matrix elements in Eq. (A5c), one has to use the three Euler angles carrying some coordinate frame, in which $\mathbf{x}_{nn'}$ is fixed, into a new, symmetry-equivalent one such that the rotated vector $\mathbf{x}_{nn'}$ coincides with $R\mathbf{x}_{nn'}$. The behavior of the spherical harmonics under complex conjugation yields a fourth property,

$$G_{nn',lm,l'm'} = (-1)^{l+l'+m+m'} G^{*}_{nn',l-m,l'-m'}. \tag{A5d}$$

Equations (A5) are translated to the Fourier transformed matrices $\mathbf{S}(\mathbf{q}) = 4\pi\, \mathbf{G}(\mathbf{q})$ [see Eqs. (23) and (28)] due to

$$S_{\lambda\lambda'}(\mathbf{q}) = S^{*}_{\lambda'\lambda}(\mathbf{q}), \tag{A6a}$$

$$S_{\lambda\lambda'}(\mathbf{q}) = (-1)^{l+l'} S_{\lambda\lambda'}(-\mathbf{q}), \tag{A6b}$$

$$S_{lm,l'm'}(R\mathbf{q}) = \sum_{m''m'''} D^{l}_{mm''}(R) D^{l'^{*}}_{m'm'''}(R) S_{lm'',l'm'''}(\mathbf{q}), \tag{A6c}$$

$$S_{lm,l'm'}(\mathbf{q}) = (-1)^{l+l'+m+m'} S^{*}_{l-m,l'-m'}(-\mathbf{q}). \tag{A6d}$$

Equation (A6a) demonstrates that $\mathbf{S}(\mathbf{q})$ is Hermitian, but $\mathbf{G}_{nn'}$ in general is not.

The symmetry of the particles can bring about extra characteristics of the matrix elements [8,13]. For axially symmetric particles with inversion symmetry, which are fixed with their inversion centers to the lattice, $G^{(d)}_{nn'}(\Omega,\Omega') = G^{(d)}_{nn'}(-\Omega,\Omega') = G^{(d)}_{nn'}(\Omega,-\Omega') = G^{(d)}_{nn'}(-\Omega,-\Omega')$ is valid, and the self-part fulfills $G^{(s)}_{nn}(\Omega,\Omega') = G^{(s)}_{nn}(-\Omega,-\Omega')$. Consequently, $\mathbf{G}^{(s)}_{nn}$ can have nonzero elements for l and l' even or for l and l' odd, respectively, while $\mathbf{G}^{(d)}_{nn'}$ has nontrivial elements for l and l' even, only.

We want to conclude this section with the remark for cubic lattices, that by symmetry the knowledge of the correlation functions for only $\frac{1}{48}$ of all lattice vectors or $\frac{1}{48}$ of the volume of the first Brillouin zone is necessary to calculate the correlations for the complete lattice or Brillouin zone.

APPENDIX B: CALCULATION OF $D^{\circ}_{\lambda\lambda'}$, $f_{nn',\lambda\lambda'}$ AND $g_{nn',\lambda\lambda'}$

In this appendix we describe how the input quantities $D^{\circ}_{\lambda\lambda'}$ [needed for the OZ equation (31) and to determine $S_{\lambda\lambda'}(\mathbf{q})$ from Eq. (28)] and $f_{nn',\lambda\lambda'}$, $g_{nn',\lambda\lambda'}$ [needed for the PY approximation, Eq. (33)] are calculated.

λ-transforming equation (18) yields

$$D^{\circ}_{\lambda\lambda'} = d_{\lambda\lambda'} - d_{\lambda,00}\, d_{00,\lambda'} \tag{B1}$$

with

$$d_{\lambda\lambda'} = 4\pi\, i^{l'-l} \int_{S^2} \rho^{(1)}(\Omega) Y^{*}_{\lambda}(\Omega) Y_{\lambda'}(\Omega) d\Omega$$
$$= 4\pi\, i^{l'-l} (-1)^{m} \sum_{\lambda''} \left[\frac{(2l+1)(2l'+1)}{4\pi(2l''+1)} \right]^{1/2}$$
$$\times C(ll'l'',000) C(ll'l'',-mm'm'') \langle Y_{\lambda''} \rangle,$$

$$d_{00,00} = 1, \tag{B2}$$

where the product rule [2] for the spherical harmonics and $\langle Y_{\lambda} \rangle = \int d\Omega\, \rho^{(1)}(\Omega) Y_{\lambda}(\Omega)$ has been used. Since the values $\langle \hat{Y}_{\lambda} \rangle$ are obtained from the MC simulation, Eqs. (A3) allow to determine the canonical averages $\langle Y_{\lambda} \rangle$. Then, $\langle Y_{\lambda} \rangle$ is substituted into Eq. (B2), with summation truncated at $l_{\max}$. This approximate result for $d_{\lambda\lambda'}$ yields $D^{\circ}_{\lambda\lambda'}$ from Eq. (B1).

Contrary to the lattice correlation functions, $f_{nn'}(\Omega,\Omega')$ is not affected by the lattice and refers exclusively to what happens between two particles. Therefore, it is advantageous to use the r frame for the calculation of the matrix elements $f_{nn',\lambda\lambda'}$, i.e., the coordinate system in which the connecting line of the particle sites coincides with the z axis. In that frame it is $f^{r}_{nn',\lambda\lambda'} = \delta_{mm'}\, f^{r}_{nn',ll'm}$. Having calculated $f^{r}_{nn',ll'm}$ one gets

$$f_{nn',\lambda\lambda'} = \sum_{m''} D^{l}_{mm''}(R) D^{l'^{*}}_{m'm''}(R) f^{r}_{nn',ll'm''} \tag{B3}$$

similarly to Eq. (A5c). The rotation matrix R carries the cubic coordinate frame into the r frame, where $R\mathbf{x}_{nn'} = (0,0,|\mathbf{x}_{nn'}|)$. In the r frame, the matrix elements have similar properties as in Ref. [21],

$$f^{r}_{nn',lm,l'm'} = \delta_{mm'}\, f^{r}_{nn',ll'm}, \quad f^{r}_{nn',ll'm} = (-1)^{l+l'} f^{r^{*}}_{nn',ll'm},$$

$$f^{r}_{nn',ll'm} = f^{r}_{nn',ll'-m}. \tag{B4}$$

In the following, the abbreviation

$$Q_{lm}(\theta) = (-1)^{m} \left(\frac{2l+1}{4\pi} \right)^{1/2} \left[\frac{(l-m)!}{(l+m)!} \right]^{1/2} \sin\theta\, P_{lm}(\cos\theta)$$

is used, where we define

$$P_{l,-m}(\cos\theta) = (-1)^{m} \frac{(l-m)!}{(l+m)!} P_{lm}(\cos\theta)$$

to cover all possible values of m. Using $\Omega_r = (\theta_r, \phi_r)$, $\Omega'_r = (\theta'_r, \phi'_r)$, $\phi_1 = \phi'_r - \phi_r$, $\phi_2 = \phi'_r + \phi_r$, $f^{r}_{nn'}(\Omega,\Omega') \equiv f^{r}(|\mathbf{x}_{nn'}|, \theta_r, \theta'_r, \phi_1)$ (which function is 2π periodic with respect to ϕ_1) and the relations $f^{r}(|\mathbf{x}_{nn'}|, \theta_r, \theta'_r, \phi_1) = f^{r}(|\mathbf{x}_{nn'}|, \theta_r, \theta'_r, -\phi_1)$, and $f^{r}(|\mathbf{x}_{nn'}|, \theta_r, \theta'_r, \phi_1) = f^{r}(|\mathbf{x}_{nn'}|, \theta_r, \pi-\theta'_r, \pi+\phi_1) = f^{r}(|\mathbf{x}_{nn'}|, \pi-\theta_r, \theta'_r, \pi+\phi_1) = f^{r}(|\mathbf{x}_{nn'}|, \pi-\theta_r, \pi-\theta'_r, \phi_1)$ (due to the head-tail symmetry) one finally ends up with

$$f^{r}_{nn',ll'm} = 16\pi\, i^{l'-l}\int_0^{\pi}\int_0^{\pi/2}\int_0^{\pi/2} f^{r}(|\mathbf{x}_{nn'}|,\theta_r,\theta_r',\phi_1) \times Q_{lm}(\theta_r)Q_{l'm}(\theta_r')\cos(m\phi_1)d\theta_r\, d\theta_r'\, d\phi_1, \quad \text{(B5)}$$

where the Mayer function in the integrand has to be taken from Eq. (34).

The calculation of $g_{nn',\lambda\lambda'}$, $n\neq n'$, is done as follows. From Eq. (13) we get

$$g_{nn',\lambda\lambda'} = \delta_{\lambda\lambda'} + h_{nn',\lambda\lambda'}. \quad \text{(B6)}$$

The OZ equation yields $\overset{\circ}{h}_{\lambda\lambda'}(\mathbf{q})$ from which the back transform $\overset{\circ}{h}_{nn',\lambda\lambda'}$ is deduced. For the calculation of $g_{nn',\lambda\lambda'}$, however, we need $h_{nn',\lambda\lambda'}$. It is easy to prove that $h_{nn',\lambda\lambda'}$ is uniquely determined by $\overset{\circ}{h}_{nn',\lambda\lambda'}$ [20],

$$h_{nn',\lambda\lambda'} = (\delta_{\lambda\lambda''} - \delta_{\lambda,00}\, d_{00,\lambda''})\overset{\circ}{h}_{nn',\lambda''\lambda'''}(\delta_{\lambda'''\lambda'} - \delta_{00,\lambda'}\, d_{\lambda''',00}), \quad \text{(B7)}$$

where summation convention is assumed. Taking $d_{\lambda\lambda'}$ from Eq. (B2), $\overset{\circ}{h}_{nn',\lambda\lambda'}$ from the OZ equation and again truncating summations at $l=l_{\max}$, Eq. (B7) yields an approximation for $h_{nn',\lambda\lambda'}$.

APPENDIX C: THE ITERATION SCHEME

The iteration scheme for solving the OZ/PY equations self-consistently will be described in this appendix. For particles of inversion symmetry, only the (ll' even) matrix elements do not vanish *a priori*. Qualitatively the scheme is similar to that for liquids, but in detail it is much more involved.

1. Step. As initial condition, which is the *preliminary* first iteration denoted by $(\tilde{\mathbf{c}}_{nn'})^{(1)}$, it is chosen

$$(\tilde{\mathbf{c}}_{nn'})^{(1)} = \begin{cases} \mathbf{0}, & n = n' \\ \mathbf{f}_{nn'}, & n \neq n'. \end{cases} \quad \text{(C1)}$$

Fourier transformation yields $\mathbf{(\tilde{c}(q))}^{(1)}$ and $\mathbf{(\tilde{c}^{\circ}(q))}^{(1)}$ by eliminating the first row and column. Now let us assume we have found $\mathbf{(\tilde{c}(q))}^{(\nu)}$ and its back transform $(\tilde{\mathbf{c}}_{nn'})^{(\nu)}$.

2. Step. Substituting $\mathbf{(\tilde{c}^{\circ}(q))}^{(\nu)}$ into the OZ equation (31) yields the total correlation function denoted by $\mathbf{(\tilde{h}^{\circ}(q))}^{(\nu)}$. Its back transform $(\tilde{\mathbf{h}}^{\circ}_{nn'})^{(\nu)}$ will not fulfill Eq. (29) in general. Therefore one has to use

$$\mathbf{(h^{\circ}(q))}^{(\nu)} = \mathbf{(\tilde{h}^{\circ}(q))}^{(\nu)} - \frac{1}{N}\sum_{\mathbf{q}} \mathbf{(\tilde{h}^{\circ}(q))}^{(\nu)} \quad \text{(C2)}$$

from which one gets $(\mathbf{h}^{\circ}_{nn'})^{(\nu)}$ and $(\mathbf{g}_{nn'})^{(\nu)}$ by use of Eqs. (B6) and (B7).

3. Step. We substitute $\mathbf{(h^{\circ}(q))}^{(\nu)}$ into the OZ equation. The resulting direct correlation function after back transformation is denoted by $(\tilde{\tilde{\mathbf{c}}}^{\circ}_{nn'})^{(\nu)}$. Finally, the *preliminary* νth iteration $(\tilde{\mathbf{c}}_{nn'})^{(\nu)}$ is replaced by the *final* one,

$$(\mathbf{c}_{nn'})^{(\nu)} = \begin{cases} \alpha(\tilde{\tilde{\mathbf{c}}}^{\circ}_{nn})^{(\nu)} + (1-\alpha)(\tilde{\mathbf{c}}^{\circ}_{nn})^{(\nu)}, & n = n' \\ (\tilde{\mathbf{c}}_{nn'})^{(\nu)}, & n \neq n', \end{cases} \quad \text{(C3)}$$

where α is a mixing parameter.

4. Step. Now one substitutes $(\mathbf{g}_{nn'})^{(\nu)}$, $(\mathbf{c}_{nn'})^{(\nu)}$, and $\mathbf{f}_{nn'}$ into the right-hand side of the PY equation (36) for $n\neq n'$ and obtains $(\mathbf{c}^{\mathrm{PY}}_{nn'})^{(\nu+1)}$. Then the *preliminary* $(\nu+1)$th iteration $(\tilde{\mathbf{c}}_{nn'})^{(\nu+1)}$ is obtained from

$$(\tilde{\mathbf{c}}_{nn'})^{(\nu+1)} = \begin{cases} (\mathbf{c}^{\circ}_{nn})^{(\nu)}, & n = n' \\ \alpha(\mathbf{c}^{\mathrm{PY}}_{nn'})^{(\nu+1)} + (1-\alpha)(\mathbf{c}_{nn'})^{(\nu)}, & n \neq n'. \end{cases} \quad \text{(C4)}$$

This procedure is repeated until a fix point for the matrices has been reached. Typically, $\alpha=0.1$ is chosen to avoid divergence. Convergence is assumed if all elements of $(\tilde{\mathbf{h}}^{\circ}_{nn})^{(\nu)}$ have submerged a certain threshold, which is chosen to be 10^{-13} times the maximum absolute value of any matrix element $(\tilde{h}^{\circ}_{nn',\lambda\lambda'})^{(\nu)}$. Additionally, the average of all nonzero matrix elements of $(\tilde{\mathbf{c}}_{nn'})^{(\nu+1)}-(\tilde{\mathbf{c}}_{nn'})^{(\nu)}$ must be below α times a second threshold, which is calculated in the same manner as the h threshold, but by taking also the $l=0$, $l'=0$ matrix elements into account.

[1] J.-P. Hansen and I. R. McDonald, *Theory of Simple Liquids*, 2nd ed. (Academic, San Diego, 1990).
[2] C. G. Gray and K. E. Gubbins, *Theory of Molecular Fluids* (Clarendon Press, Oxford, 1984), Vol. 1.
[3] J. Ram, R. C. Singh, and Y. Singh, Phys. Rev. E **49**, 5117 (1994).
[4] M. Letz and A. Latz, Phys. Rev. E **60**, 5865 (1999).
[5] J. D. Wright, *Molecular Crystals* (Cambrigde University Press, Cambridge, 2001).
[6] *The Plastically Crystalline State*, edited by J. N. Sherwood (Wiley, Chichester, 1979).
[7] M. H. Müser, D. Löding, P. Nielaba, and K. Binder, Ferroelectrics **208**, 293 (1998).
[8] R. M. Lynden- Bell and K. H. Michel, Rev. Mod. Phys. **66**, 721 (1994).
[9] H. M. James and T. A. Keenan, J. Chem. Phys. **31**, 12 (1959).
[10] A. Hüller and W. Press, in Ref. [6].
[11] T. Yamamoto, Y. Kataoka, and K. Okada, J. Chem. Phys. **66**, 2701 (1977).
[12] W. G. Hoover and F. H. Ree, J. Chem. Phys. **49**, 3609 (1968).
[13] M. Yvinec and R. M. Pick, J. Phys. (Paris) **41**, 1045 (1980); **41**, 1053 (1980).
[14] W. Breymann and R. M. Pick, Europhys. Lett. **6**, 227 (1988).
[15] W. Breymann and R. M. Pick, J. Chem. Phys. **91**, 3119 (1989); **100**, 2232 (1994).
[16] M. Descamps and G. Coulon, Chem. Phys. **25**, 117 (1977); G. Coulon and M. Descamps, J. Phys. C **13**, 945 (1980); **13**, 2847 (1980).

[17] M. Descamps and G. Coulon, J. Phys. C **14**, 2297 (1981); M. Descamps, *ibid.* **15**, 7265 (1982).
[18] A. Hüller and W. Press, Phys. Rev. Lett. **29**, 266 (1972).
[19] D. M. Kroll and K. H. Michel, Phys. Rev. B **15**, 1136 (1977).
[20] M. Ricker and R. Schilling, e-print cond-mat/0311253; M. Ricker, Ph.D. thesis, University of Mainz.
[21] R. Schilling and T. Scheidsteger, Phys. Rev. E **56**, 2932 (1997).
[22] T. Franosch, M. Fuchs, W. Götze, M. R. Mayr, and A. P. Singh, Phys. Rev. E **56**, 5659 (1997).
[23] J. Vieillard- Baron, J. Chem. Phys. **56**, 4729 (1972).
[24] A. Saupe, Z. Naturforsch. A **19A**, 161 (1964).
[25] C. Renner, H. Löwen, and J. L. Barrat, Phys. Rev. E **52**, 5091 (1995).
[26] D. Frenkel, B. M. Mulder, and J. P. Mc Tague, Phys. Rev. Lett. **52**, 287 (1984).
[27] J. K. Percus, Phys. Rev. Lett. **8**, 462 (1962).
[28] F. C. von der Lage and H. A. Bethe, Phys. Rev. **71**, 612 (1947).